Colloid Polym Sci (2008) 286:67–77
DOI 10.1007/s00396-007-1702-0

ORIGINAL CONTRIBUTION

Synthesis and direct interactions of silver colloidal nanoparticles with pollutant gases

Rita Patakfalvi · David Diaz · Donaji Velasco-Arias · Geonel Rodriguez-Gattorno · Patricia Santiago-Jacinto

Received: 9 February 2007 / Revised: 9 May 2007 / Accepted: 26 May 2007 / Published online: 21 June 2007

Abstract Silver nanoparticles (NPs) were synthesized in organic solvents. Spontaneous reduction of silver salts takes place in *N*,*N*′-dimethyl formamide (DMF) and dimethyl sulfoxide (DMSO) at room temperature. The formed colloids are not stable without a stabilizing agent, hence rarely used, and inexpensive organic molecules (β-cyclodextrin and cholic acid) were used as surface modifiers in DMF. The stabilization was successful; the Ag NPs remained stable for more than 3 months. Additionally, Ag NPs were prepared using Ag-2-ethylhexanoate and Na-citrate as capping agent in DMSO. The resulting NPs are stable, of 4.4 nm average size, and at the same time reactive for catalytic purposes. The interaction of Ag NPs with pollutant atmospheric gases (NO and SO_2) was studied. UV–visible spectra show the oxidation of silver and the very efficient reduction of NO at room temperature. SO_2 molecules are adsorbed on the NPs surface, causing their aggregation and precipitation.

Keywords Ag nanoparticles · Application · UV–vis absorbance spectroscopy · NO · SO_2

R. Patakfalvi · D. Diaz (✉) · D. Velasco-Arias · G. Rodriguez-Gattorno
Facultad de Química, Universidad Nacional Autónoma de México. Coyoacán,
04510 Mexico D.F., Mexico
e-mail: david@servidor.unam.mx

P. Santiago-Jacinto
Instituto de Física, Universidad Nacional Autónoma de México. Coyoacán,
04510 Mexico D.F., Mexico

Present address:
G. Rodriguez-Gattorno
Centro de Investigaciones Avanzadas del IPN,
Merida 97310 Yucatán, Mexico

Introduction

Among the colloidal metal particles, silver is one of the most studied metals due to its physical and chemical properties and applications. Silver exhibits unique optical properties, which are strongly dependent on the size and shape of the particles [1–3]. Analytical applications are also based on the characteristic surface plasmon absorption band of Ag nanoparticles (NPs). Its absorbance maximum position depends on the surface charge and environment of the nanoparticles; therefore, Ag NPs are used as sensors [4]. Silver nanoparticles play important roles as substrate for surface-enhanced Raman spectroscopy [5–7] and in the field of catalysis [8–10]. The microbicide properties of silver and silver cation are well known. Recently, Ag NPs were successfully tested against *Escherichia coli* and other bacteria [11–13].

In our work, the nanoparticles were prepared in polar organic solvents, such as *N*,*N*′-dimethyl formamide and dimethyl sulfoxide. The main advantage of these solvents in our synthesis pathway is that they also act as a reducing agent of the silver cations, so the number of the reactants and the reaction byproducts diminish [14, 15]. DMSO and DMF are very good solvents for nanoparticle preparation [14–19] due to their specific chemical and physical properties. Their relatively high dielectric constants allow charge separation; they are good solvents for ionic solids and polar and polarizable molecules [20]. DMSO has higher viscosity than water, so the diffusion of the particles in this solvent is slower, decreasing the number of collisions between particles, and also diminishes the particle aggregation and sedimentation processes.

As the formed NPs in DMSO or DMF are not stable without capping agents [21], we tested rarely used inexpensive organic molecules, cholic acid and β-cyclodextrin, as

stabilizer agents of the NPs. The cyclodextrins are produced by a simple enzymatic conversion process from starch [22]. β-cyclodextrin has seven α-1,4-linked gluco-pyranose units forming a truncated cone with hydrophilic outer rims and a hydrophobic cavity (Fig. 1a). The diameter of the larger rim is 1.53 nm, and the corresponding cavity diameter is 0.78 nm. Due to these properties, cyclodextrins are able to include a great variety of molecules [22, 23]. Although the hydroxylic groups are poor electrodonor ligands to silver, in relatively high concentrations, β-cyclodextrin is able to stabilize Ag NPs.

Cholic acid is one of the bile acids in humans; it is produced in the liver from cholesterol [24]. It is composed of a steroidal unit with a carboxylic acid and three hydroxyl groups (Fig. 1b). In this way, bile salts contain hydrophilic and hydrophobic components. Due to this amphiphilic character, bile acids can dissolve fats. The use of cholic acid as a nanoparticle stabilizer is not so common. In our best knowledge, just one paper has been published where a cholic acid salt was used for emulsion formation and for stabilization of magnetite particles [25]. We supposed that cholic acid might be a good stabilizer for Ag nanoparticles due to the presence of one carboxyl group.

In other experiments, silver-2-ethylhexanoate was used as silver precursor. The 2-ethylhexanoate ions also play a role in the stabilizing process [16].

In this paper, we show potential applications of the prepared Ag NPs, particularly their interactions with NO and SO_2 gases. These gases are quite soluble in DMSO. The solubility of NO in DMSO is 3×10^{-3} mol/l (25 °C) [26] and that of SO_2 is 0.582 mol/l (25 °C) [27]. Therefore, due to the great solubility of both gases in DMSO, it is possible to carry out the direct chemical interactions of Ag NPs with NO and SO_2 in colloidal dispersions.

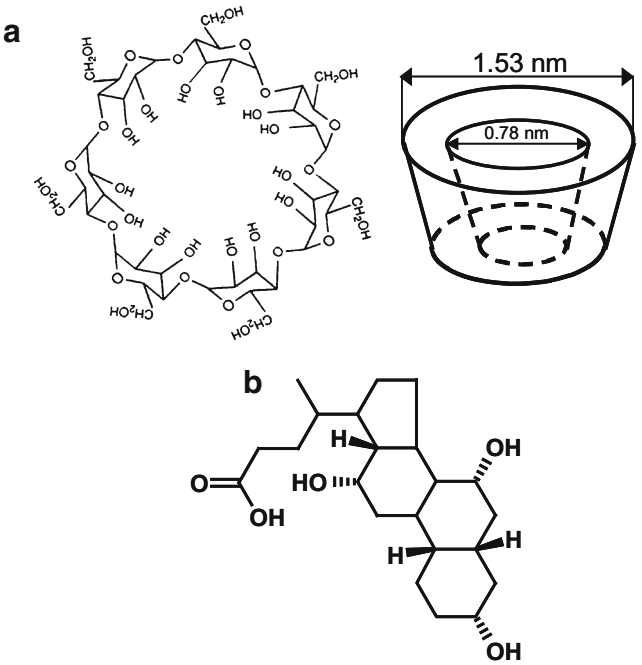

Fig. 1 The structure of β-cyclodextrin (**a**) and cholic acid (**b**)

Materials and methods

Materials Silver nitrate ($AgNO_3$, Aldrich, 99%) and silver 2-ethylhexanoate (Ag(ethex), Strem Chemical, 99%), as starting salts, were used for the Ag NPs preparation. The solvents were *N*,*N*′-dimethylformamide (DMF, Baker, 99.9%) and dimethylsulfoxide (DMSO, Baker, 99.9%). These solvents were heated at 80 °C for 40 min and bubbled with prepurified Ar gas (PRAXAIR, 99.999%) before used.

β-cyclodextrin (β-CD, $C_{42}H_{70}O_{35}$, AMAIZO), cholic acid (CA, $C_{24}H_{40}O_5$, Aldrich, 98%), and dihydrated trisodium citrate ($Na_3Cit{\cdot}2H_2O$, Aldrich, 99%) were used as stabilizing agents.

$NaNO_2$ (Baker, 99.99%), $FeSO_4{\cdot}7H_2O$ (Baker, 99.6%), H_2SO_4 (Baker) and Na_2SO_3 (Mallinckrodt, 99.02%) were used to generate NO and SO_2 gases. Ultrapure water (18 MΩ cm^{-1}) was obtained from a Barnstead E-pure deionization system. All chemical reagents were used in their commercial form without further purification.

Methods UV–vis absorption spectra were collected in an Ocean Optics CHEM2000 fiber optic spectrophotometer. High-resolution transmission electron micrographs (HRTEM) were obtained using a JEM FASTEM 2010 instrument equipped with a HAADF detector for Z-contrast imaging operating at 200 kV and a JEOL 4000EX at 400 kV. Fast Fourier transform of HRTEM micrograph images was done by means of DigitalMicrograph™ GATAN v-3.7.0. software. X-ray diffraction (XRD) measurements were registered on a Siemens D5000 equipment using Cu Kα radiation (20 mA, 40 kV, λ=1.5418 Å). For the XRD study, Ag NPs were synthesized in high concentration (10^{-2} M Ag and 10^{-1} M β-cyclodextrin). The samples were centrifuged at 3,000 rpm for 20 min, washed with water three times and finally with acetone, and dried. The surface electric potentials were measured in a Mütek PCD 03 particle charge detector.

Preparation methods

Ag NPs synthesis

1. For the silver NPs synthesis, an appropriate amount of β-cyclodextrin (concentration range, 5×10^{-4}–7.5×10^{-2} M) was mixed with DMF (50 ml, previously bubbled with argon). After solving the β-CD, an adequate amount of $AgNO_3$ was added to the reaction

solution under vigorous stirring. The initial colorless solution became yellowish after 10 min, which is an indication of Ag NPs formation.

2. The synthesis using cholic acid was similar to the previous case. A suitable amount of cholic acid (5×10^{-2} M) was dissolved in DMF. After the complete dissolution of cholic acid, $AgNO_3$ (5×10^{-4} M) was added to the solution. The effect of the reaction temperature on the formed NPs was studied at 25, 40, 50, and 60 °C.
3. A corresponding quantity of Na_3Cit was dissolved in a minimum amount of water and then taken into 50 ml of DMSO (previously saturated with Ar). Ag(ethex) (final concentration 10^{-4} M) was added to the solution under vigorous stirring. The solution was heated at 60 °C for 20 min. The same method was applied to obtain 2×10^{-4} M Ag NPs, which were used to test their catalytic activity.

Ag NPs application

Experiments of Ag colloid dispersion interactions with NO and SO_2 were carried out in a sealed UV-visible cell filled with 3 ml of a 2.5×10^{-4} M Ag dispersion. NO was generated from the reaction between $FeSO_4$ and $NaNO_2$ [28]. SO_2 gas was synthesized using Na_2SO_3 and H_2SO_4. The gas and silver dispersions were dried with previously activated Linde 4-Å molecular sieves at 500 °C for 16 h. NO and SO_2 gases were flushed with an argon gas flow of 0.6 l/min to the cell. The quantity of NO and SO_2 were controlled by careful addition of known quantities of $FeSO_4$ or H_2SO_4, over the $NaNO_2$ or Na_2SO_3 salts, respectively.

Results and discussion

Synthesis of Ag NPs in DMF using β-cyclodextrin as stabilizing agent

The reduction of Ag(I) ions takes place spontaneously in DMF according to the following reaction [14]:

$$HCONMe_2 + 2Ag^+ + H_2O \rightarrow 2Ag^0 + Me_2NCOOH + 2H^+$$

At high temperature, the carbamic acid easily decomposes:

$$Me_2NCOOH \rightarrow CO_2 + Me_2NH$$

A silver mirror is formed on the beaker walls when any stabilizing agent is absent in the reaction medium. Therefore, in the first experiments, β-cyclodextrin was used as stabilizing agent. β-cyclodextrin solubility in DMF is high, $(9.08\pm2)\times10^{-2}$ M [29]; accordingly, we can use highly concentrated β-cyclodextrin solutions.

The formation and stability of the silver particles were monitored by UV–vis absorption spectroscopy looking for the characteristic resonance surface plasmon band of the silver NPs. Ag(I) concentration was firstly optimized during the synthesis. It was observed that 5×10^{-4} M $AgNO_3$ concentration was the optimal concentration. At lower Ag (I) concentration (10^{-4} M), the particles were aggregated, and Ag mirror formation was also observed on the beaker walls. The UV–vis spectra of these samples showed a decrease of the absorption after 2 h, indicating Ag(0) precipitation. When Ag(I) concentration is high, for example 10^{-3} M, the mirror development was not observed, although the shape of the resonance surface plasmon band indicated the presence of larger particles.

The effect of the [Ag(I)]/[β-CD] concentration ratio on the stability and particle size was also investigated. Although the reduction of Ag(I) by DMF takes place at room temperature, when β-cyclodextrin was in solution, the UV–vis spectra showed a slow particle formation (Fig. 2, the sample concentration was too high to measure real spectra; in that case, the sols were diluted four times with DMF). A period of 5 to 12 days is necessary to reach the final chemical equilibrium, depending on the β-CD concentration. The Ag(I) reduction rate was increased with temperature. However, heating also favored the silver mirror formation. Therefore, we chose to work at room temperature during the Ag NPs synthesis.

When the [Ag(I)]/[β-CD] concentration ratios are [1]:[10] or [1]:[50], the sols exhibit high stability even after 40 days (Fig. 2b). The shape of the spectra is symmetric with narrow half width, which suggests a particle narrow size distribution. However, we have to remark that after 40 days, Ag deposit on the glass walls was also observed. Furthermore, when the [Ag(I)]/[β-CD] concentration ratios are [1]:[1], [1]:[100], or [1]:[150], the synthesized Ag NPs are not stable, and silver aggregation is observed in all cases (Fig. 2a,c).

Comparing the spectral data of the Ag NPs after 12 days, we can see the dependence of the size and stability on the β-cyclodextrin concentration. In the case of the two most stable sols ([Ag(I)]/[β-CD]=1:10 or 1:50), the absorption maximum (417, 419 nm), together with a very small plasmon band half width mean (79, 90 nm), suggest the presence of uniform and small Ag NPs. When the [Ag(I)]/[β-CD] concentration ratios are 1:1, 1:100, or 1:150, that is, when the Ag sols are not stable, the plasmon resonance band is shifted toward longer wavelengths, suggesting particle agglomeration. We also observed a broadening of the resonance surface plasmon band, and this is an indication of a wider particle size distribution.

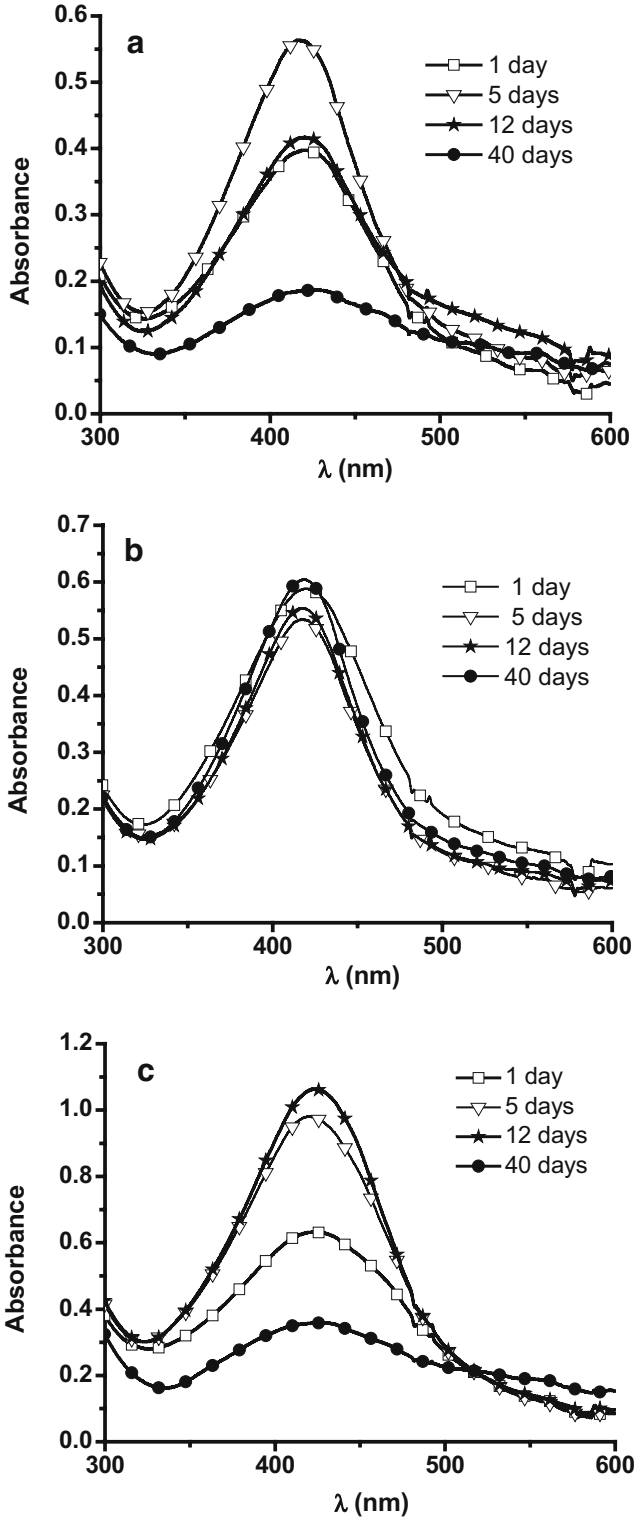

Fig. 2 Time evolution of the UV–vis electronic absorption spectra during the Ag NPs synthesis in DMF with **a** [Ag(I)]/[β-CD]=1:1, **b** 1:10, and **c** 1:150 (the sols were diluted four times with DMF)

The presence of the Ag nanoparticles was also confirmed by XRD measurements in solid samples. The XRD patterns showed the formation of Ag NPs with cubic phase (Fig. 3).

The particle size was determined by TEM measurements; the average size was 7.2 nm (Fig. 4).

Synthesis of Ag NPs in DMF using cholic acid as stabilizing agent

The Ag NPs formation was followed by electronic absorption UV–vis spectroscopy. The Ag(I) reduction process was very slow at room temperature. The particle formation was observed only after 2 h when the characteristic color of the silver colloids appears. This is the reason why the reaction temperature was increased. We used the following temperatures: 25, 40, 50, and 60 °C, using a water bath and heating for 2 h, in every case. It is well known that the Ostwald's particle ripening process is favored at high temperatures. Therefore, we did not want to try higher temperatures. Increasing the temperature from 25 to 40 °C had no important effect on the reaction rate. Higher temperatures, such as 50 and 60 °C, accelerated the process, and after 30 min, particle formation was evident when the colorless solution became yellowish. But even at these high temperatures, the reaction rate was relatively slow. We can see in Fig. 5a the changes of the absorption maxima with time. It is worth mentioning that no aggregation or silver deposit on the beaker glass wall was observed after 40 days. The values of the absorption maxima increase with temperature. Absorbance differences among the various sols are still evident even after 40 days. Again, this suggests that the reaction rate is very slow; consequently, longer time is required to reach the equilibrium.

At higher temperatures, the surface plasmon resonance band shifts towards lower wavelengths: λ_{max} (25 °C, 40 days)=417 nm, λ_{max} (60 °C, 40 days)=411 nm (Fig. 5b).

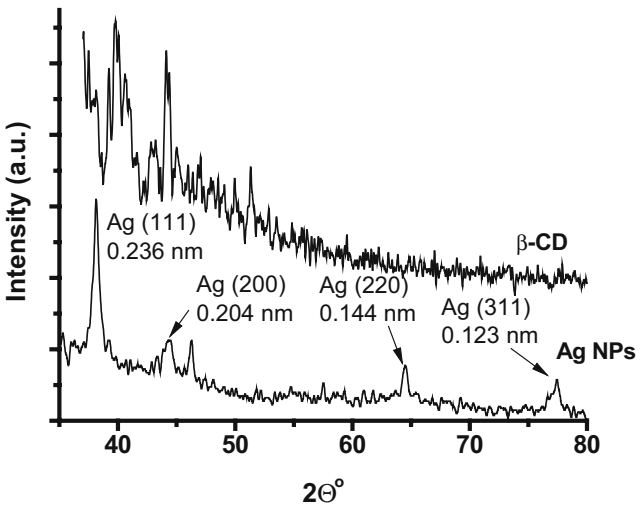

Fig. 3 X-ray diffraction patterns of pure β-cyclodextrin and Ag NPs stabilized with β-cyclodextrin ([$AgNO_3$]=10^{-2} M, [β-CD]=10^{-1} M)

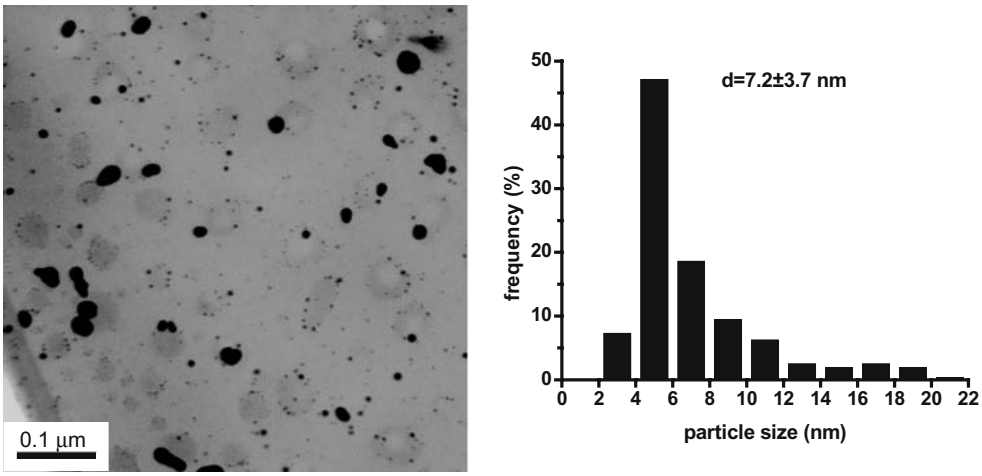

Fig. 4 TEM image and size distribution of β-CD stabilized Ag NPs ([Ag(I)]/[β-CD]=1:50)

At the same time, the half width value of that band also becomes narrower. This is an indication of smaller particles with a narrow size distribution. We suggest that this is due to the higher reduction rate, which favors the formation of small nucleus. If the nucleation rate process is faster than the particle growth, smaller particles will be formed [30]. It is also worth to mention that the 68 nm value for the half width (in the case of the Ag sol prepared at 60 °C) is an indication of the presence of monodisperse nanoparticles [31].

The comparison of the spectral time evolution shows very well that the reaction at the highest temperature is also slow (Fig. 6a). The spectra were measured in a 1-mm quartz cuvette because the absorbance values were too high. It was observed that the surface plasmon resonance band increased after more than 3 months. It is also important to point out that the plasmon band maximum shifts towards smaller wavelength values. This spectral behavior is indicative of the formation of smaller clusters from agglomerated particles, as was mentioned before. The new clusters are stabilized by the carboxyl group of the cholic acid. The plasmon band shape is very symmetric and narrow, suggesting that the particle size distribution is also very narrow.

These results suggested to carry out the synthesis for a longer heating time; therefore, the experiments were repeated using the same $AgNO_3$ and cholic acid concentrations, and the reaction temperature (60 °C) was fixed for 1, 2, 3 or 4 h.

The effect of the heating time on the particle formation rate followed by UV–vis spectroscopy can be observed in Fig. 6b. The reaction rate increases with the heating time. However, after 5 h, there is no significant difference between the 2, 3 and 4 h samples. It suggests that it is not necessary to heat for more than 2 h.

The particle size was determined by TEM and STEM modes for the most stable sample (heating time 60 °C during 2 h). The micrographs showed a bimodal size distribution (Fig. 7a). There was a fraction with very small (3.7 nm average size) Ag nanoparticles and another with larger particles (20.8 nm average size). HRTEM images also confirmed the presence of Ag(0) NPs with cubic phase. Figure 7b shows the characteristic Fast Fourier transform of cubic Ag NPs obtained by image processing through Digital image software.

Synthesis of Ag NPs in DMSO with Ag(ethex) and Na-citrate

Ag NPs were also prepared in DMSO using Ag(ethex) as precursor. DMSO spontaneously reduces this silver salt to elemental silver:

$$2[\mathrm{AgOOCR}] + (\mathrm{CH_3})_2\mathrm{SO} : + \mathrm{H_2O} \rightarrow 2Ag^0 + (\mathrm{CH_3})_2\mathrm{SO_2} + 2\mathrm{H}^+ + 2[: \mathrm{OOCR}]^- R = -(\mathrm{C_2H_5})\mathrm{CH}(\mathrm{CH_2})_3\mathrm{CH_3}$$

According to the suggested reaction mechanism, the first step is the complexation of the $(CH_3)_2SO$: to the metal ion species:

$$[\mathrm{AgOOCR}] + (\mathrm{CH_3})_2\mathrm{SO} : \leftrightarrows \left[(\mathrm{CH_3})_2\mathrm{SOAgOOCR}\right]$$

Followed by electron transfer to form a sulfoxide radical cation:

$$\left[(\mathrm{CH_3})_2\mathrm{SOAgOOCR}\right] \rightarrow \mathrm{Ag^0} + \left[(\mathrm{CH_3})_2\mathrm{SO}^\bullet\right]^+ + [: \mathrm{OOCR}]^-$$

Which then transfers a second electron:

$$\left[(\mathrm{CH_3})_2\mathrm{SO}^\bullet\right]^+ + [\mathrm{AgOOCR}] \rightarrow \left[(\mathrm{CH_3})_2\mathrm{SO}\right]^{2+} + \mathrm{Ag^0} + [: \mathrm{OOCR}]^-$$

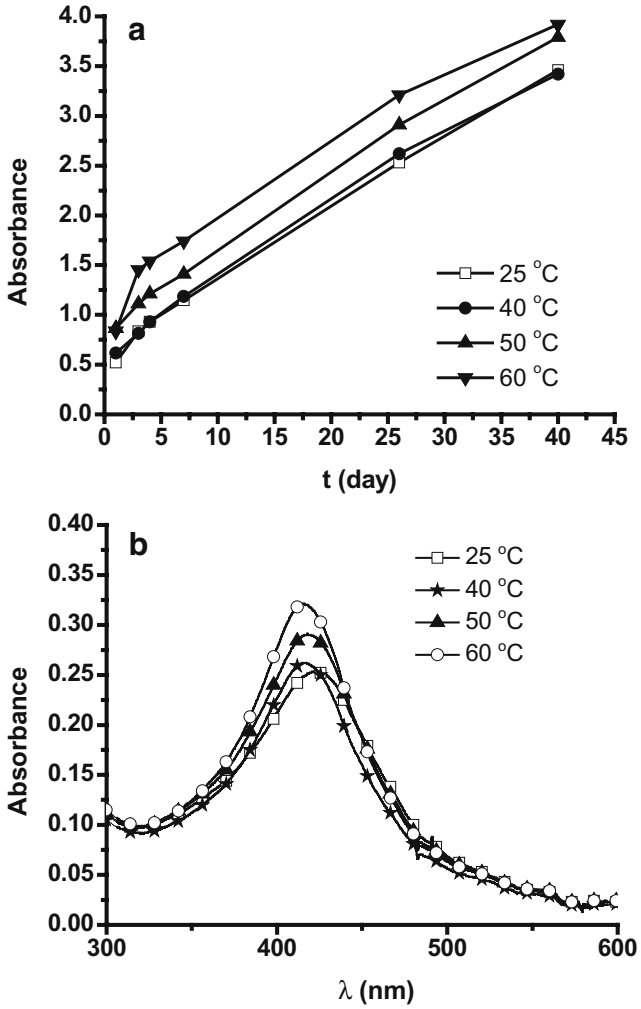

Fig. 5 **a** Effect of the reaction temperature on the Ag NPs formation. Plot of the time evolution of the absorbance of Ag colloids at 425 nm ([$AgNO_3$]=5×10^{-4} M and [CA]=5×10^{-2} M, the spectra of 16 and 40 days were measured in 10-mm cuvette, and the data were adjusted to 10-cm cuvette by Beer–Lambert's law); **b** UV–vis spectra of Ag NPs prepared at different temperatures after 40 days (measuring in 10-mm cuvette)

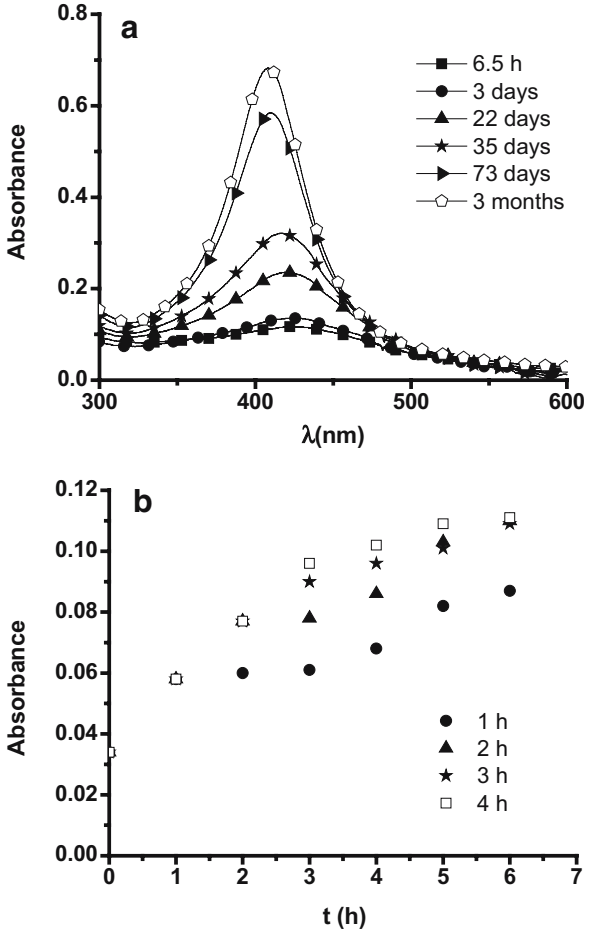

Fig. 6 **a** Time evolution of the UV–vis absorption spectra during the Ag NPs synthesis at 60 °C ([$AgNO_3$]=5×10^{-4} M and [CA]=5×10^{-2} M; the sample was measured in a 1-mm cuvette); **b** The effect of heating time at 60 °C on the CA-Ag NPs formation: plot of the absorbance at 425 nm ([$AgNO_3$]=5×10^{-4} M and [CA]=5×10^{-2} M)

Therefore, the cationic species is attacked by water forming the sulfone:

$$\left[(CH_3)_2SO\right]^{2+} + H_2O \rightarrow [CH_3)_2SOOH_2]^{2+} \rightarrow (CH_3)_2SO_2 + 2H^+$$

Other transition metals are used to oxidize sulfoxides to sulfones in the same way [32].

The characteristic yellowish color of silver colloids signed the NPs formation after 10–15 min at room temperature in the DMSO–Ag(ethex) solution. The time evolution spectra show that the reduction process is slow (Fig. 8a). After 4 h, the intensity of the plasmon band does not change significantly, but the half width at the maximum of the plasmon band is wider. After 24 h, a precipitate can be observed, suggesting that the spectrum broadening is a result of an increment in particle size or to an agglomeration process. Increasing the temperature can accelerate the reduction process, but the nanoparticle agglomeration is also favored.

As this colloid dispersion was not stable, we decided to use Na-citrate as capping agent, as trisodium citrate is a commonly applied silver stabilizer [33]. The capping agent is added at the beginning of the reaction to disperse the NPs before they grow. A disadvantage of Na-citrate is its low solubility in DMSO. Hence, we dissolved it in one drop of water and increased the reaction temperature to 60 °C for 20 min to allow a better solubility of Na-citrate and the rapid formation of silver nucleus. Under these conditions, the reduction of Ag(ethex) would proceed via a simultaneous and cooperative reaction with DMSO and citrate ions.

Figure 8b shows the UV–visible spectra at different times during the formation of Ag NPs in DMSO using Ag(ethex) (1×10^{-4} M) and Na-citrate (1×10^{-4} M). The stability of these NPs is outstanding, as they remain stable for more than 8 months: The Na-citrate and 2-ethylhexanoate molecules, together, successfully stabilize the formed Ag NPs. The

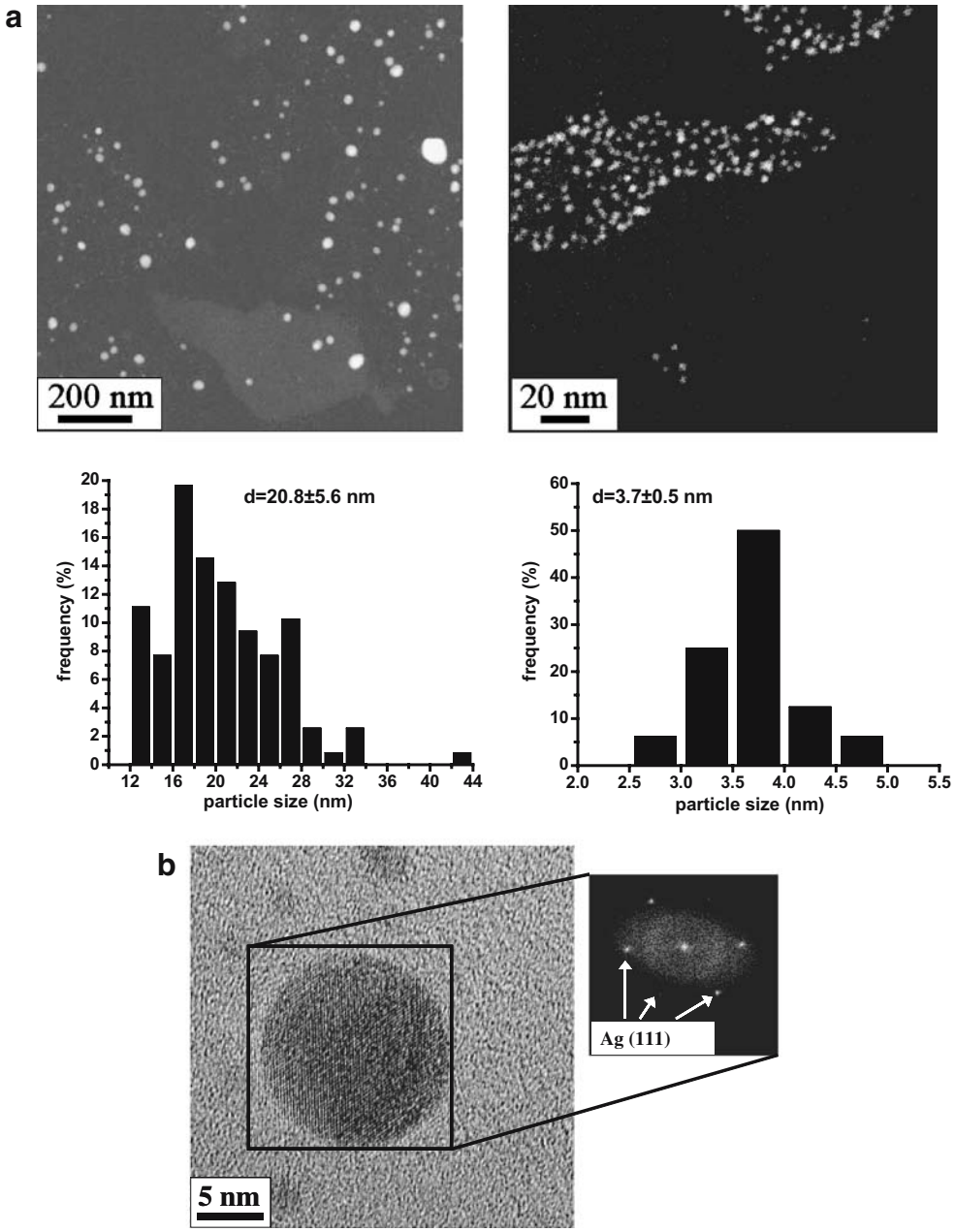

Fig. 7 **a** HAADF-TEM micrographs and bimodal size distribution of Ag-cholic acid sample and **b** HRTEM image of one Ag nanoparticle. The *inset* shows the corresponding FFT obtained by image processing using Digital Micrograph software. The reflections agree with the values of the silver cubic structure (reaction condition, 5×10^{-4} M $AgNO_3$, 5×10^{-2} M cholic acid in DMF, 2 h, 60 °C)

stabilization effect of citrate molecules was confirmed by measuring the NPs surface electric potential. Without Na-citrate, when only 2-ethylhexanoate ions cover the NPs surface, the electric potential is −100 mV. However, using citrate ions, the measured surface potential is −200 mV. This potential creates a sufficient repulsive force between NPs to avoid particle aggregation.

Figure 9 shows Z-contrast image of this Ag dispersion measured after 11 days. Roughly, spherical NPs can be observed with 4.4±1.2 nm average size. The HR-TEM studies of different samples show that particle size distribution is essentially the same in the range for silver concentration from 1×10^{-4} M to 5×10^{-3} M.

Interaction of Ag NPs with NO

Very stable Ag NPs have been synthesized. It was an important question to evaluate their catalytic activity. The direct interaction between the Ag NPs and NO was firstly studied. Nitric oxide is an acidic species; NO in water generates an acidic solution, which leads to spontaneous agglomeration of Ag NPs. To remove any trace of water in the reaction system and to keep NO gas and Ag colloids dry, pretreated 4-Å molecular sieves was utilized. Therefore, we used anhydrous silver nanoparticle dispersions and dried NO gas. The Ag NPs and NO interaction experiment was performed several times with very good reproducibility.

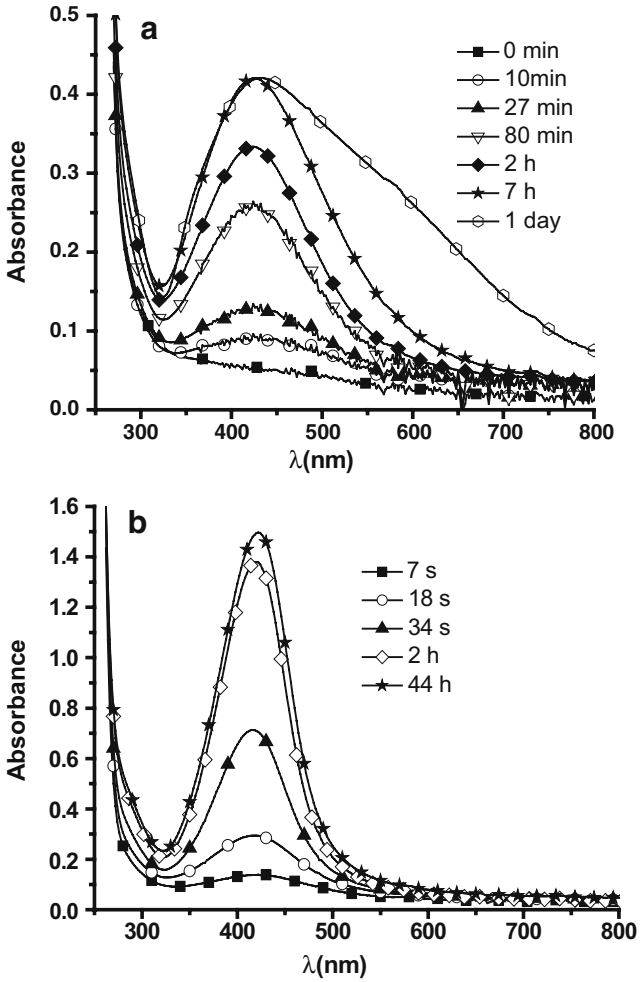

Fig. 8 **a** Time evolution of the UV–Vis electronic absorption spectra during the Ag NPs synthesis in DMSO with Ag(ethex) (1×10^{-4} M) at room temperature and **b** using Ag(ethex) (1×10^{-4} M) and sodium citrate (1×10^{-4} M) heated at 60 °C for 20 min

Figure 10a and b shows the electronic absorption spectra of NO gas in DMSO at different concentrations and reacting with silver under anhydrous reaction conditions. The Ag(I) concentration was 2.5×10^{-4} M in these experiments, allowing the collection of several spectra on consecutive additions of NO. The plasmon resonance band decreases proportionally with each NO addition because the Ag NPs immediately react with NO until the Ag metal is completely dissolved. After six additions of NO, the typical spectrum of NO arises as result of its excess after completed dissolution of metallic silver. The presence of Ag(I) ions in the remaining solution was confirmed. It is worth to mention that the Ag NPs are not regenerated upon heating these previously used dispersions.

It was not possible to determine the NO and Ag stoichiometric coefficients accurately because the NO concentration was not accurately known. However, it is possible to make a very good estimation of the amount of generated NO during each addition. If we suppose that the NO conversion is always 100% in every addition, we can calculate approximately the Ag(0)/NO ratio in the reaction. The area under plasmon band is proportional to the particle number concentration (taking into account that particle sizes remain essentially the same, i.e., band position and the half width at the maximum does not change); hence, assuming that Ag(ethex) reduction is quantitative, the area under plasmon band can be associated to the amount of Ag (0) which was not consumed in the reaction. The area under the plasmon resonance band is shown as a function of the amount of NO after every addition (Fig. 10c). As we can see, there is a linear dependence between the reacted silver and the conversion of NO. As the original concentration of Ag dispersion was 2.5×10^{-4} M and 0.003 l was used in this experiment, the total amount of silver which was reacted with NO was 7.5×10^{-7} mol. As the total amount of NO was 4.4×10^{-4} mol, it means that every silver atom transformed 587 NO molecules. This suggests that reaction of NO with silver NPs takes place through a catalytic process, while the oxidation of colloidal metallic silver occurs as a secondary reaction. The most probable products are N_2O, O_2, and N_2 according to the following reactions as

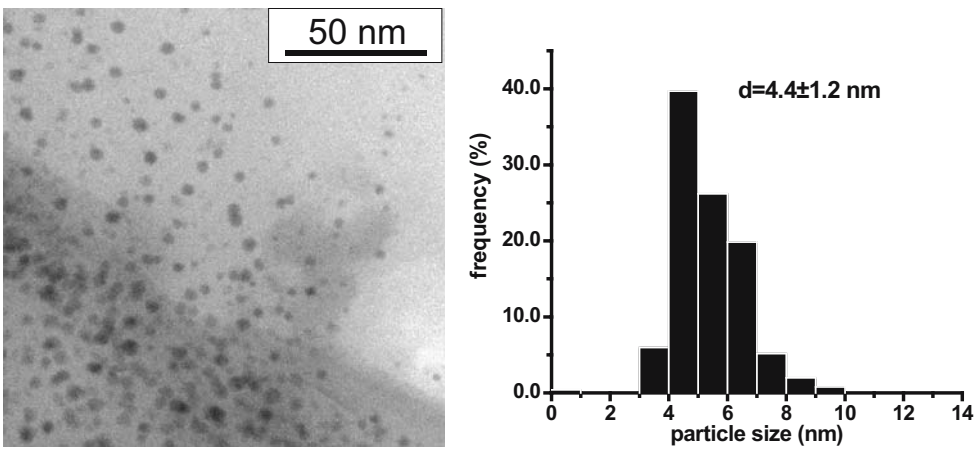

Fig. 9 Conventional TEM micrograph and size distribution of the citrate- and 2-ethylhexanoate stabilized Ag NPs in DMSO from Ag(ethex)

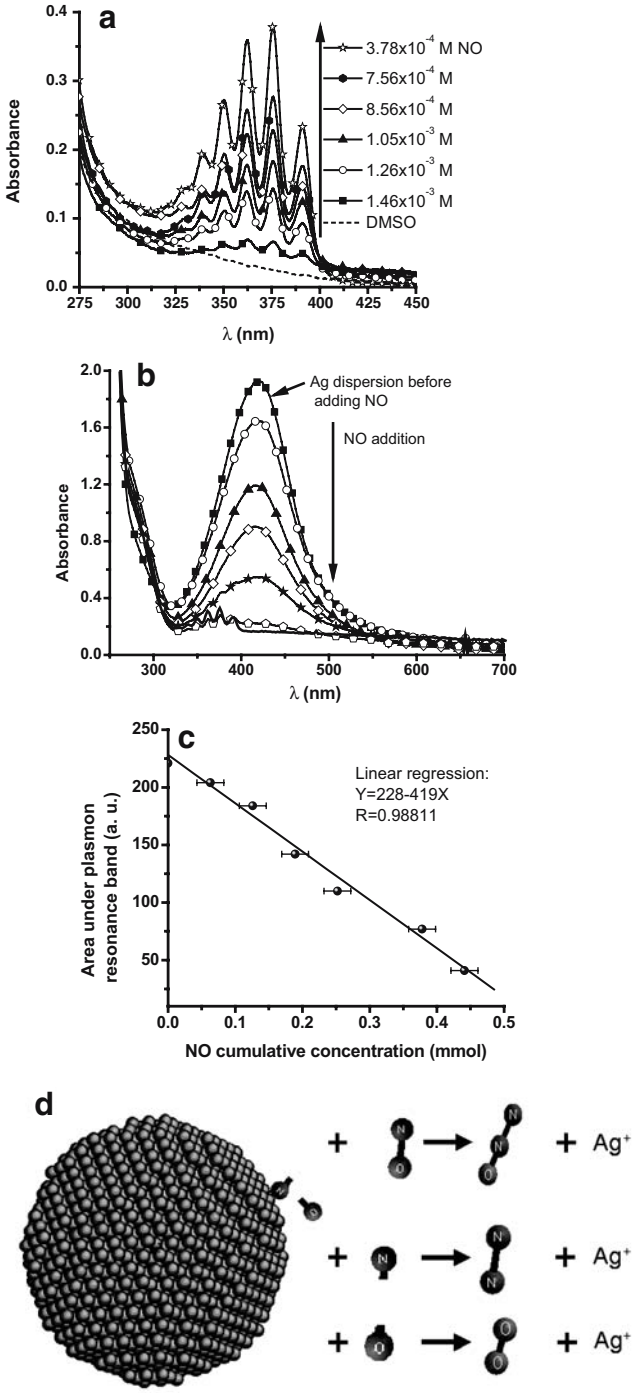

Fig. 10 **a** Electronic absorption spectrum of NO dissolved in anhydrous DMSO; **b** electronic absorption spectra of Ag NPs (2×10^{-4} M) after additions of equal quantities of NO; **c** area under the plasmon resonance band as a function of the amount of NO in every addition; **d** schematic mechanism of the catalytic process of NO degradation on Ag surface

previously reported in studies of NO dissociation over metallic silver (Fig. 10d) [34–36]:

1. $Ag_n + NO \leftrightarrows [Ag_n - N - O]$
2. $[Ag_n - N - O] \leftrightarrows [Ag_n - N - - - O]$
3. $[Ag_n - N - - - O] \leftrightarrows N + O + Ag_n$
4. $N + N \rightarrow N_2$
   $O + O \rightarrow O_2$
   $N + NO \rightarrow N_2\,O.$

Interaction of Ag NPs with SO_2

The direct interaction between the Ag NPs and SO_2 solved in DMSO was studied. SO_2 is a chemical species with more acid character than NO. The silver concentration of these experiments was also 2.5×10^{-4} M and were accomplished under anhydrous reaction conditions. Figure 11a shows the absorption spectra of the dissolved SO_2 in DMSO with different concentrations and reacting with silver NPs (Fig. 11b). We can see that the surface plasmon resonance band decreases with the addition of up to 4.427 mmol SO_2, and, at the same time, the spectrum of SO_2 appears. After 1 day, aggregation and precipitation of metallic silver was observed.

According to the geochemical classification of the elements, silver is a calcophilic element, so it has a great affinity towards sulfur. Taking into account the electronic configurations of the reacting species, the HOMO and LUMO molecular orbitals of the SO_2 molecule are localized in the sulfur atom, which suggests that the bonds of SO_2 will arise from this site. Haase [37] has studied the interaction of silver with SO_2 and suggested that the SO_2–Ag bond arises from the interaction between the HOMO and LUMO orbitals of SO_2 and the 5s and 5p orbitals of silver.

The synthesized Ag NPs are stabilized with 2-ethylhexanoate and citrate ions, which are in dynamical equilibrium with the solvent molecules on the NPs surface. As the 2-ethylhexanoate molecules are not strongly bonded to the silver surface, they might be exchanged by SO_2 molecules. The adsorbed SO_2 molecules can cause the aggregation and precipitation of the silver NPs as shown in the spectrum in Fig. 11b. The 2-ethylhexanoate and citrate anions cause a negative surface electric potential. These anions are displaced by SO_2 molecules; therefore, the original electric potential decreases, changing to a more positive value. This change in potential favors the aggregation of the Ag particles (Fig. 11c).

Conclusions

Ag nanoparticles were prepared in dimethylformamide and dimethyl sulfoxide. The formation and the stability of the particle were monitored by UV–vis spectroscopy looking for the characteristic resonance surface plasmon band of the silver nanoparticles.

The reduction of Ag(I) ions takes place spontaneously in DMF. In the first experiments, β-cyclodextrin was used as

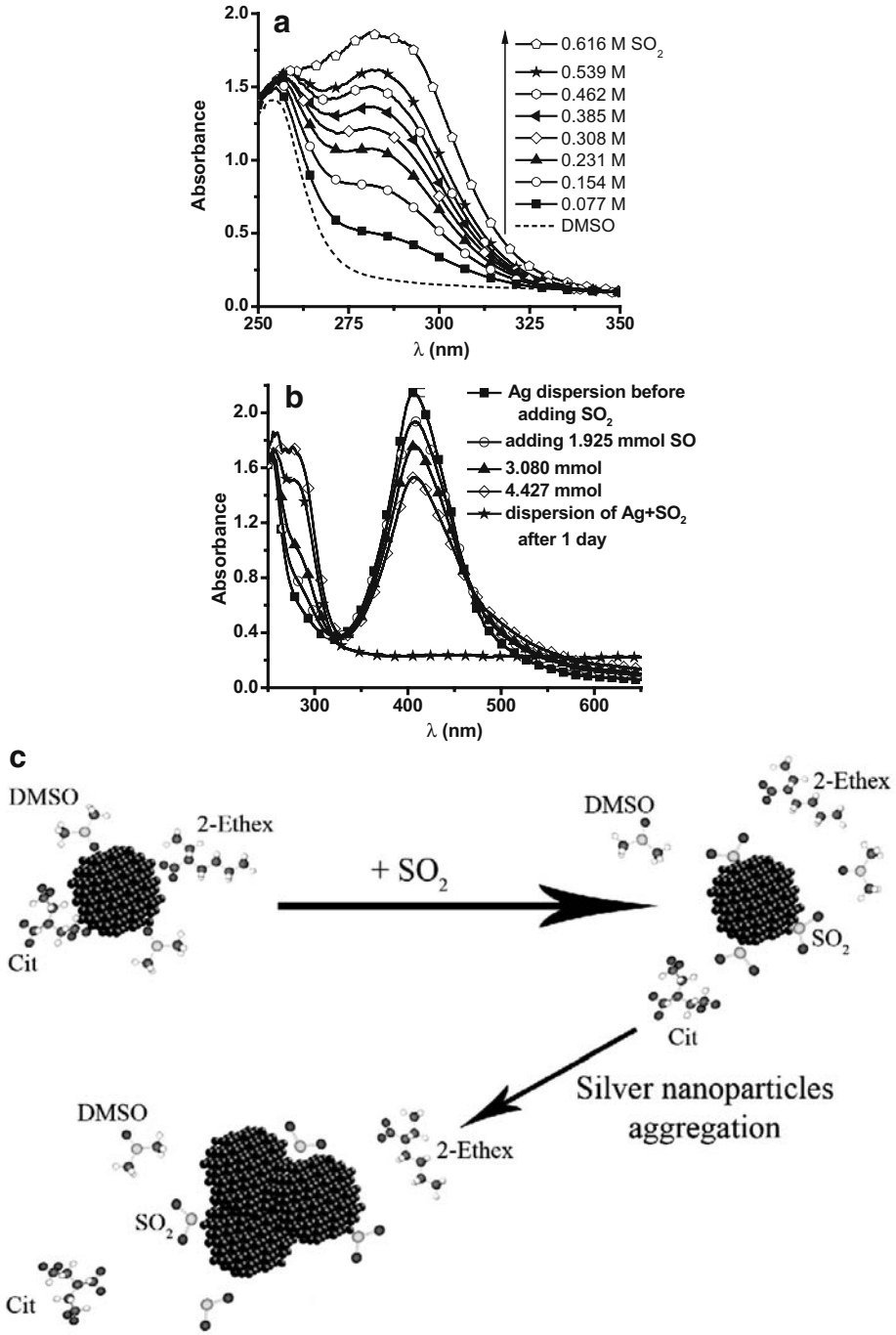

Fig. 11 **a** Absorption electronic spectra of SO_2 in DMSO at different concentrations; **b** electronic absorption spectra of Ag NPs (2×10^{-4} M) after additions of different quantities of SO_2; **c** schematic mechanism of the interaction between Ag NPs and SO_2 molecules

stabilizing agent. After optimizing the Ag(I) concentration during the synthesis, the effect of the [Ag(I)]/[cyclodextrin] concentration ratio was also determined. Stable nanoparticles were obtained with this capping agent. According to the TEM micrograph measurements, particles of 7.2 nm average size were formed. The particles were stable even after 1.5 months.

We tested cholic acid as a stabilizer for Ag nanoparticles via the carboxyl group. The effect of the reaction temperature and the heating time for stable particle formation were studied. Higher temperatures favored the formation of smaller particles. Cholic acid has been demonstrated to be a very good capping agent: Very stable Ag NPs were synthesized with a bimodal size distribution. The smaller fraction has a 3.7-nm average size.

Ag NPs of average diameter close to 4.4 nm and narrow size distribution were prepared by the addition of silver 2-ethylhexanoate to DMSO in the presence of Na-citrate as stabilizer. We tested the potential catalytic properties of these colloidal silver nanoparticles under normal reaction conditions. UV–visible spectra show that silver NPs in

DMSO react fast with NO under anhydrous conditions, causing the dissolution of metal. At the beginning of the Ag NPs and NO interaction, a very efficient catalytic process for the NO chemical reduction takes place. Then, occurs the Ag NPs disintegration leading to the Ag(I) ion dissolution.

The interaction between Ag NPs and SO_2 was also studied. SO_2 molecules adsorbed onto the colloid surface change their negative electric potential to a more positive potential, leading to the aggregation of the silver particles.

Acknowledgments R.P. gives thanks to DGAPA UNAM for the post-doc fellowship. We also thank L. Rendon for HRTEM observation assistance. The authors are also thankful to the Central Microscopy facilities of the Institute of Physics, UNAM. D.D. wants to thank CONACyT E43662 and DGAPA UNAM IN110405 for financial support. Finally, the authors want to thank Dr. M. Iglesias-Arteaga for providing us cholic acid.

References

1. Liz-Marzán LM (2006) Langmuir 22:32
2. Evanoff DD Jr, Chumanov G (2005) ChemPhysChem 6:1221
3. Okada N, Hamanaka Y, Nakamura A, Pastoriza-Santos I, Liz-Marzán LM (2004) J Phys Chem B 108:8751
4. Riboh JC, Haes AJ, McFarland AD, Yonzon CR, van Duyne RP (2003) J Phys Chem B 107:1772
5. Shirtcliffe N, Nickel U, Schneider S (1999) J Colloid Interface Sci 211:122
6. Nickel U, Castell A, Pöppl K, Schneider S (2000) Langmuir 16:9087
7. Bright RM, Musick MD, Natan MJ (1998) Langmuir 14:5695
8. Shiraishi Y, Toshima N (1999) J Mol Catal A 141:187
9. Keshavarajal A, She X, Flytzani-Stephanopoulos M (2000) Appl Catal B 27:L1
10. Dobosz A, Sobczynski A (2003) Water Res 37:1489
11. Sondi I, Salopek-Sondi B (2004) J Colloid Interface Sci 275:177
12. Jain P, Pradeep T (2005) Biotechnol Bioeng 90:59
13. Yeo SY, Lee HJ, Jeong SH (2003) J Mater Sci 38:2143
14. Pastoriza-Santos I, Liz-Marzán LM (1999) Langmuir 15:948
15. Rodríguez-Gattorno G, Díaz D, Rendón-Vázquez L, Hernández-Segura OG (2002) J Phys Chem B 106:2482
16. Díaz D, Rivera M, Ni T, Rodríguez JC, Castillo-Blum SE, Nagesha D, Robles J, Álvarez-Fregoso OJ, Kotov NA (1999) J Phys Chem B 103:9854
17. Rodríguez-Gattorno G, Santiago-Jacinto P, Rendon-Vázquez L, Németh J, Dékány I, Díaz D (2003) J Phys Chem B 107:12597
18. Díaz D, Castillo-Blum SE, Álvarez-Fregoso O, Rodríguez-Gattorno G, Santiago-Jacinto P, Rendon L, Ortiz-Frade L, León-Paredes YJ (2005) J Phys Chem B 109:22715
19. Zamudio A, Elías AL, Rodríguez-Manzo JA, López-Urías F, Rodríguez-Gattorno G, Lupo F, Rühle M, Smith DJ, Terrones H, Díaz D, Terrones M (2006) Small 3:346
20. Parker AJ (1965) In: Raphael RA, Taylor EC, Wynnberg H (eds) Advances in organic chemistry. Wiley Interscience, New York, pp 1–46
21. Pastoriza-Santos I, Serre-Rodríguez C, Liz-Marzán LM (2000) J Colloid Interface Sci 221:236
22. Szejtli J (2004) Cyclodextrins and molecular encapsulation. In: Nalwa HS (ed) Encyclopedia of nanoscience and nanotechnology, vol 2. American Scientific Publishers, pp 283–304
23. Szejtli J (1998) Chem Rev 98:1743
24. Navas Díaz A, García Sánchez F, García Pareja A (1998) Colloids Surf A 142:27
25. Landfester K, Ramírez LP (2003) J Phys Condens Matter 15:S1345
26. Ascenzi P, Frutero R, Ercolani C, Monacelli F (1996) Analysis 24:318
27. Li H, Liu DZ, Wang FA (2002) J Chem Eng Data 47:772
28. Bruce King R (1994) Encyclopedia of inorganic chemistry. Wiley, New York
29. Danil de Namor AF, Traboulssi R, Lewis DFV (1990) J Am Chem Soc 112:8442
30. Shaw DJ (1980) Introduction to colloid and surface chemistry. Butterworths, London
31. Wang W, Chen X, Efrima S (1999) J Phys Chem B 103:7238
32. Hoyle J (1988) Oxidation of sulphoxides and sulphones. In: Patai S, Rappoport Z, Stirling C (eds) The chemistry of sulphones and sulphoxides. Wiley, New York, p 969
33. Henglein A, Giersig M (1999) J Phys Chem B 103:9533
34. Carley AF, Davies PR, Roberts MW, Santra AK, Thomas KK (1998) Surf Sci 406:L587
35. Rodríguez JA (1990) Surf Sci 226:104
36. Citra A, Andrews L (2001) J Phys Chem A 105:3042
37. Haase J (1997) J Phys Condens Matter 9:3647